

PLANS for ELECTRON BERNSTEIN WAVES EMISSION DETECTION in COMPASS*

J. Preinhaelter¹, V. Fuchs¹, J. Urban¹, J. Zajac¹

¹EURATOM/IPP.CR Association, Prague, Czech Republic

Introduction

Last year the COMPASS-D tokamak was transferred from UKAEA Culham to the Institute of Plasma Physics Prague. A new 16 channel radiometer will be available for detecting electron cyclotron emission (ECE) from the first harmonic in the frequency range 26-40 GHz and from the second harmonic in the frequency range 60-90 GHz, supposing a low magnetic field scenario ($B_0 \leq 1.3$ T on axis). For a central density in the $5 \times 10^{19} \text{ m}^{-3}$ range the first harmonic is cut off for O- and X-mode emission and therefore only electron Bernstein waves (EBWs), converted to electromagnetic waves in the upper hybrid resonance region, can be responsible for ECE. During the last few years, we have developed a code simulating this process. The code includes a Gaussian beam antenna description, full wave O-X-EBW conversion efficiency calculation at the plasma periphery and 3D ray tracing of EBWs, including collisionless as well as collisional damping. COMPASS magnetic equilibria are computed by ACCOME [1]. These equilibria are applied for EBW simulations. We are studying conditions for the EBW-X-O conversion at oblique incidence (a remotely steered mirror is part of our antenna). Specifically, we determine the optimum angles for complete transmission of the waves through the plasma resonance. This preliminary study (the first plasma in COMPASS is planned for the end of 2008) can also determine how the radiation temperature, following from EBW emission measurements, can be used for determining the temperature profile with a very high temporal resolution.

Radiometer and antenna system

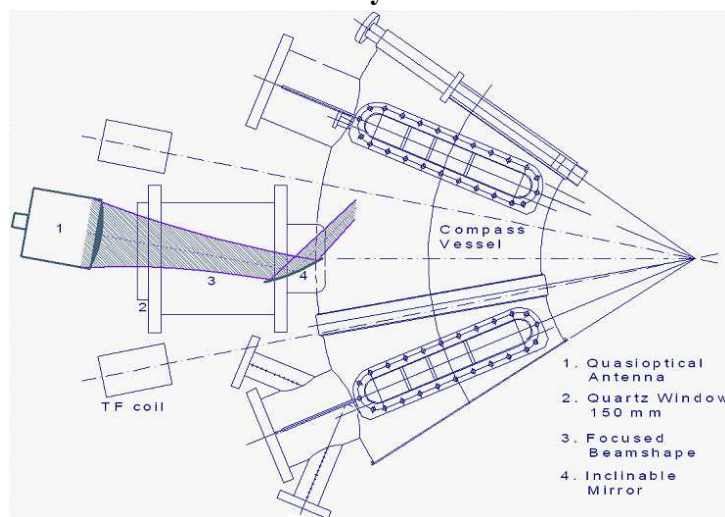


Fig 1 ECE antenna for 26-40GHz band

Our Gaussian optic lens antenna (GOLA-28/cross) is placed in front of vacuum and has two outputs to simultaneously detect both orthogonal linear polarizations. At present we have a single 16 channel receiver. Thus, we can switch between 'O' and 'X' polarizations only manually between shots. The antenna design is depicted in Fig. 1. The waist of the Gaussian beam is situated at mirror centre (4) and its diameter is 50mm. For the EBWE detection at the fundamental harmonic, a microwave front-end of 26.5 – 40 GHz will be used. The radial resolution of detected temperature will be within 1 – 2 cm with 0.875GHz bandwidth. The alternative 60-90 GHz front-end will be used for detection of direct 2nd harmonic X-mode ECE. In this case, the mirror must be removed and the antenna oriented perpendicularly to the

magnetic field. The input frequency will be either 60 – 73.5 GHz or 76.5 – 90 GHz depending on the input filter which suppresses the parasitic side-band.

EBWE simulation

In low magnetic field regime, plasma in COMPASS is usually overdense for the 1st harmonic O- and X- modes. Thus, electron cyclotron emission is possible only if we consider

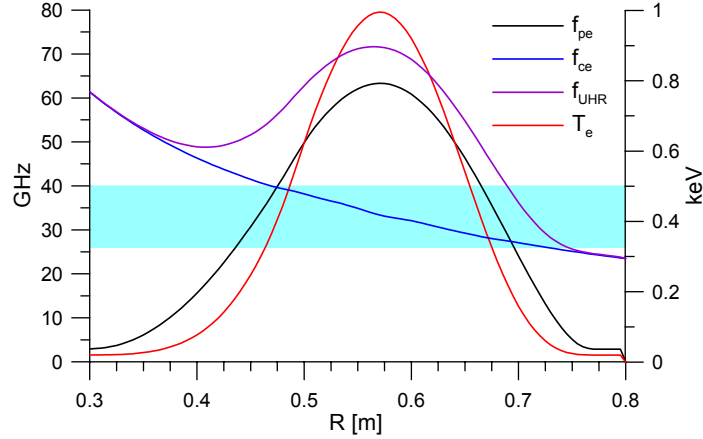


Fig. 2. Radial profiles of electron plasma frequency f_{pe} , electron cyclotron frequency f_{ce} , upper hybrid frequency f_{UHR} , and electron temperature T_e . COMPASS SND 1.2 T equilibrium computed by ACCOME.

conversion of the electrostatic EBWs in the upper hybrid resonance to transverse electromagnetic modes. Actual experimental data, particularly MHD equilibrium and electron density and temperature profiles, are not now available for COMPASS. Therefore, we use magnetic equilibrium results from ACCOME [1] modelling and assume analytically determined density and temperature profiles, plotted in Fig. 2. Assuming a central density $n_0 = 5 \times 10^{19} m^{-3}$, central temperature $T_0 = 1 \text{keV}$ and an on-axis magnetic field $B_0 = 1.2 \text{T}$, we see that the

emission from the 1st harmonic fits well in the 26-40GHz band of our radiometer.

In Fig. 3, the positions of electron cyclotron resonances for several frequencies (vertical lines) are plotted in the poloidal cross-section of magnetic surfaces. The local temperature detected by the radiometer (if we neglect the reabsorption along the rays) is determined by the positions where rays are emitted. Actually, in the code, rays are launched at the plasma

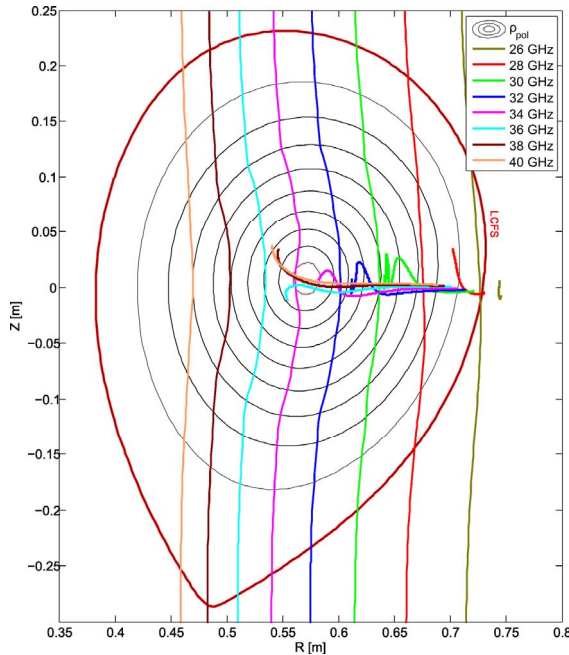


Fig. 3. Poloidal plasma cross-section of COMPASS with magnetic surfaces. Central ray trajectories for various frequencies and their respective electron cyclotron resonances are depicted.

boundary and followed to the 99% absorption point as absorption and emission are mutually reciprocal.

The situation in determining the electron temperature in EBWE detection is further complicated by the X-O conversion process, which reduces the detected radiation intensity. The EBW-X conversion in the upper hybrid resonance is usually 100%. The dependence of the radiative temperature T_{rad} on the frequency is seen in Fig. 4. In our code [2], we replace the Gaussian beam by a set of rays and for each of them we find the spot on the plasma surface. The conversion efficiency is then determined by the full wave solution of wave equations at the vicinity of this spot and the radiative temperature follows from the ray tracing. The detected signal is

determined by the integration of T_{rad}^{ray} corresponding to individual rays, weighted by the product of conversion efficiency and the Gaussian weight, over the waist. Our radiometer detects linearly polarized wave (O-mode at oblique incidence is elliptically polarized with main axis parallel to B_0) so we can detect $\sim 60\%$ of the radiation at best. Conversion efficiency is further reduced because of the divergence of the beam (rays on the outskirts of beam do not have a direction corresponding to 100% transmission). See [3] for angular

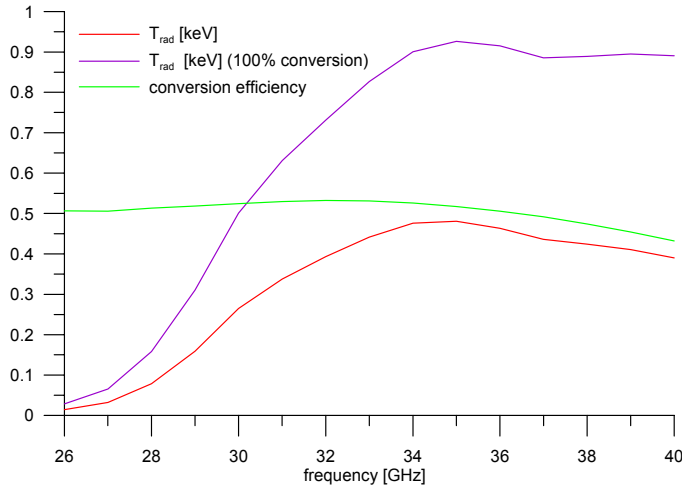


Fig. 4. Results for optimum angles $\varphi_{tor} = 36.3^\circ$, $\varphi_{pol} = -2.1^\circ$. 25 rays per beam were used and integrated in the waist plane.

requirements of optimum aiming. We characterize the antenna aiming by two angles determining the direction of the central ray: the poloidal angle φ_{pol} - an angle of the central ray with respect to the equatorial plane and the toroidal angle φ_{tor} - an angle which the projection of the central ray onto the equatorial plane makes with the vertical plane going through mirror centre and tokamak Z axis. The dependence of the conversion efficiency of O-X-EBW process on φ_{tor} and φ_{pol} is depicted in the first two rows of the contour maps in Fig. 5. We see that the region of the strong conversion shrinks as the frequency of the wave increases. The optimum poloidal angle $\varphi \approx -2^\circ$ does not depend on the wave frequency, The optimum toroidal angle shifts from 38° for 26GHz to 33° for 40GHz.. The angular dependence of the radiative temperature detected by our radiometer for different frequencies is given by the next two rows of the contour maps in Fig. 5. We see that the optimum angles for T_{rad} are determined mainly by the O-X-EBW conversion efficiency. The strongest emission is detected for the wave with $f = 36\text{GHz}$ when T_{rad} is determined by the electron temperature at the plasma centre.

Conclusions

From our simulation it follows that the radiometer and antenna system are well-suited for the detection of EBW emission from the first harmonic. In a model situation we found the optimum angles for the proper antenna aiming. We plan to use our radiometer for detecting the central temperature with very high time resolution in the similar way as it was done for NSTX [4].

dependence of transmission coefficient. We see that at 26GHz waves are emitted out of LCFS (see Fig. 3) so $T_{rad} \approx 0$. Waves with $f = 35\text{GHz}$ are emitted from the plasma centre and T_{rad} reaches a maximum of about 0.45keV. Due to the Doppler broadening of the electron cyclotron resonances, the waves with $f > 35\text{GHz}$ do not penetrate deeply to the HFS but are absorbed on the HFS near the plasma centre.

Design of antenna system in Fig. 1 is strongly influenced by the

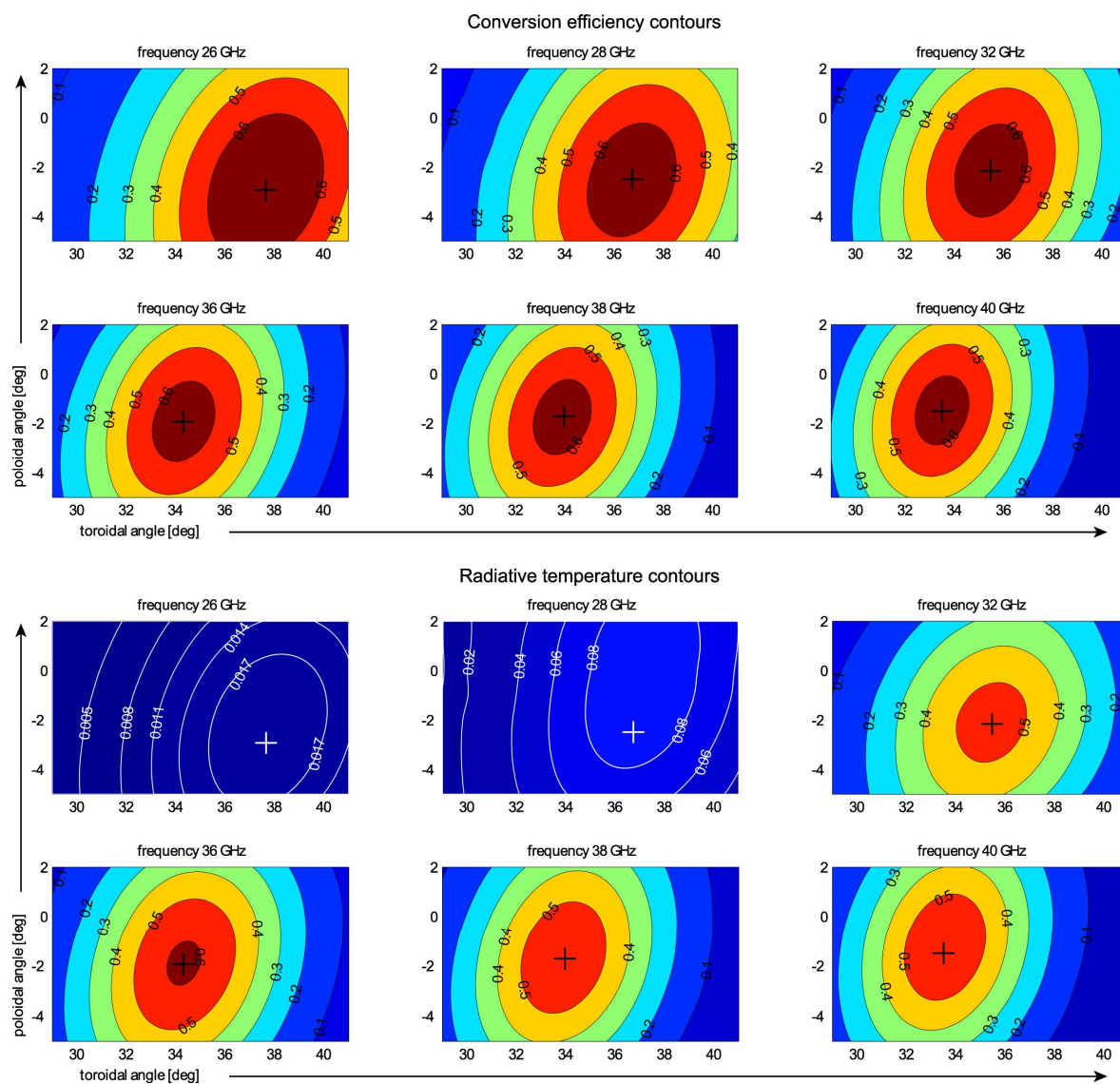


Fig. 5. Toroidal and poloidal angle scan of EBW-X-O conversion efficiency (top) and radiative temperature T_{rad} (bottom). Simulations were performed for the central rays only. Optimum angles for efficient conversion are marked by crosses.

*Partly supported by the Grant No. 202/08/0419 of Czech Science Foundation, by INTAS Ref. Nr. 05-1000008-8046 and by EURATOM.

References

- [1] V. Fuchs, et al., Heating and current drive modeling for the IPP Prague COMPASS tokamak this conference (2008).
- [2] J. Urban et al, 32nd EPS Plasma Physics Conference proceedings, Tarragona, Spain (2005).
- [3] J. Preinhaelter and V. Kopecky: V., *J. Plasma Phys.* 10, 1 (1973), part 1.
- [4] J. Preinhaelter, et al.: AIP Conference Proceedings 787, ed. Stephen J. Wukitch, Paul T. Bonoli, (2005), 349-352.